



LETTER

Remote silicate supply regulates spring phytoplankton bloom magnitude in the Gulf of MaineZhengchen Zang ^{1,*} Rubao Ji,¹ Yonggang Liu ² Changsheng Chen,³ Yun Li,⁴ Siqi Li,³ Cabell S. Davis¹¹Department of Biology, Woods Hole Oceanographic Institution, Woods Hole, Massachusetts; ²College of Marine Science, University of South Florida, St. Petersburg, Florida; ³School for Marine Science and Technology, University of Massachusetts Dartmouth, New Bedford, Massachusetts; ⁴School of Marine Science and Policy, University of Delaware, Lewes, Delaware**Scientific Significance Statement**

The spring diatom bloom in the Gulf of Maine (GoM) plays an important role in fueling the marine ecosystem and nutrient cycling, whereas the mechanism regulating its magnitude is less understood. We employed an artificial neural network method to identify the spring blooms from satellite images and reconstructed the spring bloom magnitude with strong inter-annual variability. This study provides the first evidence that the spring bloom magnitude in the central GoM is associated with the inflow of the silicate-rich deep Scotian Shelf Water due to strong silicate limitation. The results suggest that silicate limits the magnitude of spring bloom, and monitoring the proportion of deep Scotian Shelf Water in the Northeast Channel in winter and early spring can help forecast the spring bloom magnitude in the GoM.

Abstract

Spring phytoplankton blooms in the Gulf of Maine (GoM) are sensitive to climate-related local and remote forcing. Nutrient supply through the slope water intrusion has been viewed as critical in regulating the GoM spring blooms, with an assumption that nitrogen is the primary limiting nutrient. In recent years, this paradigm has been challenged, with silicate being recognized as another potential limiting nutrient, but the source of silicate and its associated water mass remain difficult to be determined. In this study, a time series of spring bloom magnitude was constructed using a self-organizing map algorithm, and then correlated with the fluctuation of water composition in the deep Northeast Channel. The results reveal the importance of silicate supply from previously less-recognized deep Scotian Shelf Water inflow. This study offers a new hypothesis for spring bloom regulation, providing a better understanding of mechanisms controlling the spring bloom magnitude in the GoM.

*Correspondence: zzang@whoi.edu**Associate editor:** Angelique White**^aAuthor Contribution Statement:** Z.Z. and R.J. developed the idea for this study. Z.Z. and Yo.L. reconstructed and analyzed the satellite data. Z.Z., Yu.L., C.C., S.L., and C.S.D. analyzed the physical model results. All authors contributed to drafting and improving the manuscript.**^bData Availability Statement:** Reconstructed 8-d composite of surface chlorophyll concentration data and metadata template for the dataset are available in the Zenodo repository at <https://doi.org/10.5281/zenodo.5077173>. The physical model (FVCOM–GOM3) products are available at NECOFS Web Map Server http://www.smast.umassd.edu:8080/thredds/catalog/models/fvcom/NECOFS/Archive/Seaplan_33_Hindcast_v1/daily_mean/catalog.html. The Matlab SOM code used in this study can be downloaded from the Github repository https://github.com/zzangwhoi/L_O_letters_Paper2021. Silicate and nitrate data used in this study are extracted from the Gulf of Maine Region Nutrient and Hydrographic Database at <http://grampus.umeoce.maine.edu/nutrients>.

Additional Supporting Information may be found in the online version of this article.

This is an open access article under the terms of the [Creative Commons Attribution](https://creativecommons.org/licenses/by/4.0/) License, which permits use, distribution and reproduction in any medium, provided the original work is properly cited.

The Gulf of Maine (GoM) is a biologically productive shelf ecosystem, receiving water flows from the Scotian Shelf and the northwest Atlantic Ocean (Bigelow 1927; Brown and Irish 1993; Smith et al. 2001). There has been strong evidence suggesting that nutrients in the GoM are supplied by Slope Water intrusion through the Northeast Channel (NEC; Ramp et al. 1985; Townsend 1998; Townsend et al. 2006). The Slope Water entering the GoM involves Warm Slope Water (WSW) from the Gulf Stream and North Atlantic Central Water and Labrador Slope Water (LSW) from the Labrador Current system (Gatien 1976). Both WSW and LSW have higher concentrations of nitrate than silicate: nitrate concentration in WSW is $\sim 24 \mu\text{M}$, which is about $8 \mu\text{M}$ higher than that in LSW; silicate concentration, however, ranges from 10 to $14 \mu\text{M}$ in both WSW and LSW (Petrie and Yeats 2000; Townsend et al. 2006). Another important deep-water mass entering the GoM is deep Scotian Shelf Water (dSSW; Hannah et al. 2001). Compared with WSW and LSW, dSSW has a high silicate concentration due to the mixing with terrestrial freshwater and the supply of regenerated silicate from the Scotian Shelf (Townsend et al. 2010). Once entering the GoM, the admixture of three water masses spills into the deep basins (Fig. 1), and it is brought to the surface by vertical mixing, Ekman upwelling, and convective overturning (Thomas et al. 2003; Rebeck and Townsend 2014; Townsend et al. 2015).

Spring phytoplankton bloom is responsible for a substantial part of the annual primary production and plays an important role in regulating the biogeochemical cycle and the productivity of higher trophic levels. In the GoM, the spring bloom timing and magnitude directly affect multiple food web components, including zooplankton (Durbin et al. 2003; Pershing and Stamieszkin, 2020), larval fish (Platt et al., 2003), and demersal fish (Townsend and Cammen,

1988). Many previous studies have confirmed that diatoms are the dominant phytoplankton group during the spring bloom in the GoM (Townsend et al. 2005, 2006; Pan et al. 2011; Turner et al. 2021; Zang et al. 2021). Canonically, the intrusion of nitrate-rich Slope Water and the ratio of LSW to WSW are viewed as critical in regulating the nutrient supply and spring bloom magnitude, with an assumption that nitrogen is the primary limiting nutrient (Schlitz and Cohen 1984; Ramp et al. 1985; Townsend 1991; Thomas et al. 2003). More recent studies, however, challenge this viewpoint and suggest the importance of silicate in regulating productivity in the GoM (Townsend et al. 2010; Switzer et al. 2020). Given roughly equal proportions of nitrate and silicate required by diatoms from waters with disproportionately lower concentrations of silicate than nitrate (Brzezinski 1985), silicate could be more limiting than nitrate for diatoms in the GoM. Thus, understanding the variations of silicate supply due to the changing deep-water components is essential in exploring the nutrient regimes in the GoM and its role in the development of the spring bloom (Townsend et al. 2006; Smith et al. 2012). Previous studies have suggested that changing water mass properties and nutrient regimes might influence phytoplankton blooms in the GoM (Thomas et al. 2003; Rebeck and Townsend 2014; Saba et al. 2015), but some key questions remain, including (1) What is the major water mass responsible for the variability of silicate supply during spring blooms? (2) Is remote supply more important than local regeneration of silicate? In this study, we integrate data from a hydrodynamic model, field measurements, and satellite observations from 2001 to 2016, aiming to quantitatively investigate the relationship between the deep-water composition and the spring bloom magnitude in the GoM.

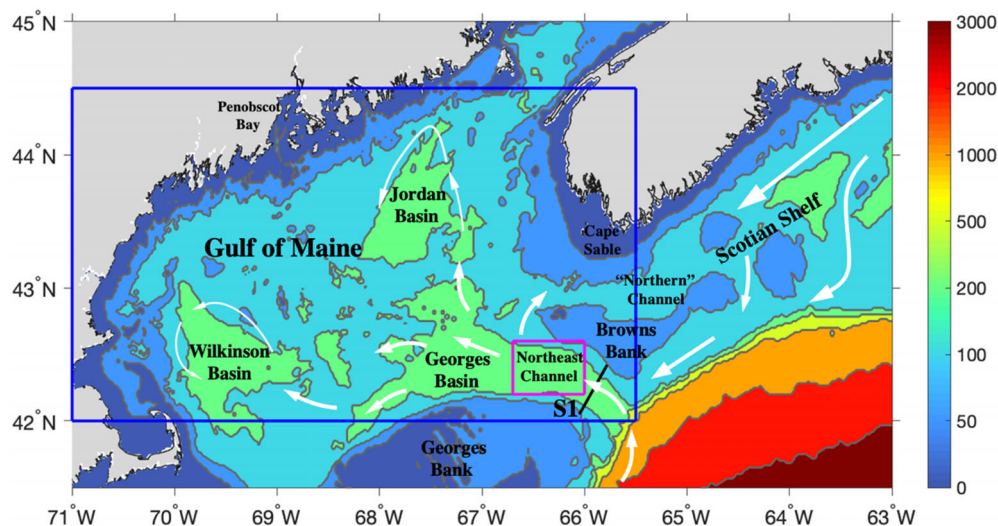


Fig. 1. Map of the GoM and surrounding regions with bathymetric contours at 50, 100, 200, 500, 1000, 2000, and 3000 m. The blue box (longitude: 65.5°W – 71°W ; latitude: 42°N – 44.5°N) indicates our study area. The white arrows represent the general circulation pattern of deep water ($> 100 \text{ m}$).

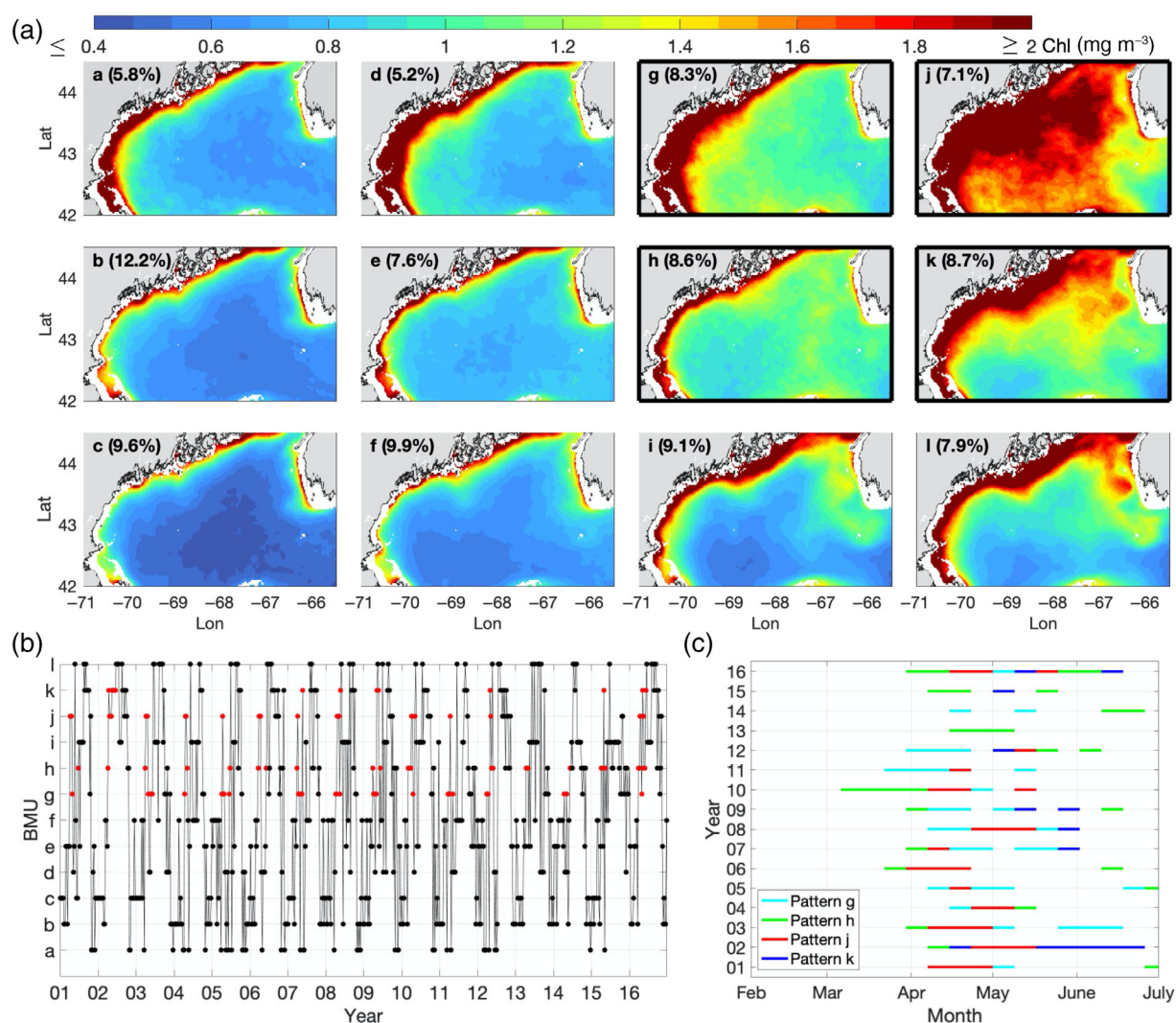


Fig. 2. Characteristic 3 \times 4 SOM patterns of surface chlorophyll concentration in the GoM (12 subpanels in **(a)**) and the time series of the Best Matching Unit (BMU; **b**) from 2001 to 2016. The occurrence frequency of each pattern is shown as a percentage in each subpanel. The bloom patterns (g, h, j, k) with high spatial averaged chlorophyll concentration ($> 1 \text{ mg m}^{-3}$) are shown in the black boxes in the upper panels, and the corresponding BMU in the time series are marked by red dots in **(b)**. **(c)** The duration and timing of bloom patterns in each year.

Data and methods

Sea surface chlorophyll, nutrients, and physical variables

Surface chlorophyll data used in this study are the 8-day composite of MODIS-terra chlorophyll products. The L3 data with a 4-km spatial resolution were extracted from 42°N to 44.5°N and 65.5°W to 71°W and interpolated onto a $0.025^\circ \times 0.025^\circ$ grid (Fig. 1). The chlorophyll data were reconstructed using the Data INterpolation Empirical Orthogonal Function (DINEOF) to fill the spatial gaps (Beckers and Rixen 2003; Alvera-Azcárate et al. 2005, 2007, 2011). Readers are referred to the Supporting Information Section S1 for more details about DINEOF. Concentrations of silicate and nitrate at the surface 20 m in the GoM from 2001 to 2016 were

extracted from the Gulf of Maine Region Nutrient and Hydrographic Database.

The physical fields used in this study are model results of Finite Volume Community Ocean Model—Gulf of Maine Version 3 (FVCOM-GOM3; Chen et al. 2003, 2011, 2021a). The model domain covers the entire GoM and adjacent regions. FVCOM-GOM3 assimilates mooring and ship measurements of temperature, salinity, and current profiles to improve the quality of model outputs (Chen et al. 2009). The results of FVCOM-GOM3 have been calibrated and applied in previous studies (Chen et al. 2011, 2021b; Sun et al. 2013, 2016; Li et al. 2015; Ji et al. 2017; Zang et al. 2021). Simulated temperature, salinity, and current velocity were interpolated onto the satellite data grid to facilitate further analysis.

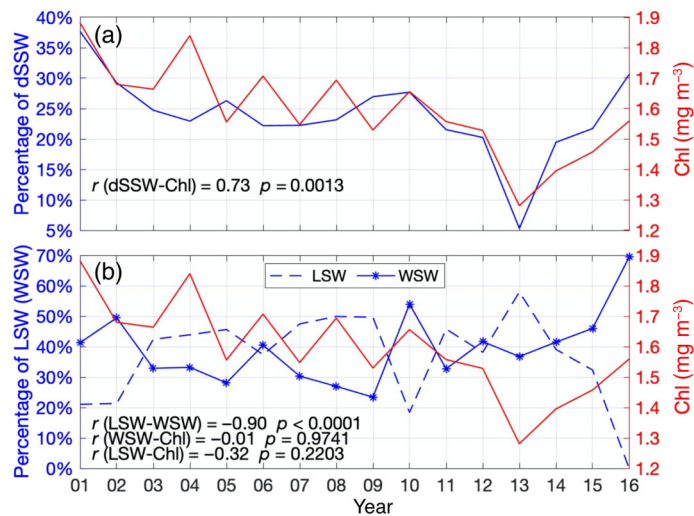


Fig. 3. (a) The interannual variations of dSSW fraction in the deep Northeast Channel (blue) and spatiotemporally averaged chlorophyll concentration during spring bloom (red) over the entire GoM; (b) The interannual variations of LSW and WSW fractions in the deep Northeast Channel (blue) and spatiotemporally averaged chlorophyll concentration during spring bloom (red).

Self-organizing map and spring bloom identification

We applied the self-organizing map (SOM) to identify spring bloom from the satellite data. As an effective tool for data clustering, the artificial neural network SOM performs a non-linear projection from the high-dimensional input data onto a low-dimensional grid (Kohonen 1982, 2001; Liu and Weisberg 2011). Here we used a flat rectangular lattice, and the size of map was specified as 3×4 following Liu and Weisberg (2005). The node weight vectors were linearly initialized, and the batch training algorithm was used to enhance the training efficiency (Liu et al. 2006, 2009, 2016). The chlorophyll data were \log_{10} normalized to alleviate the influence of coastal water with high chlorophyll (Telszewski et al. 2009). By estimating the Euclidean distance between the satellite data and the SOM patterns, a best matching unit (BMU) with the minimum distance could be found for each frame (Kohonen 2001). Therefore, all the input data were clustered into 12 patterns, and the time series of BMU showed the temporal evolution of these patterns (Fig. 2). The SOM patterns were classified into bloom and non-bloom patterns using the spatial averaged chlorophyll concentration, and those patterns with high values ($> 1 \text{ mg m}^{-3}$) were defined as bloom patterns. To minimize the impact of highly productive coastal areas, we excluded the nearshore regions with chlorophyll $> 5 \text{ mg m}^{-3}$ from the estimation. Since the bloom patterns also existed in the second half year due to the occurrence of fall bloom, only those bloom patterns appearing in the first half year were used in our analysis.

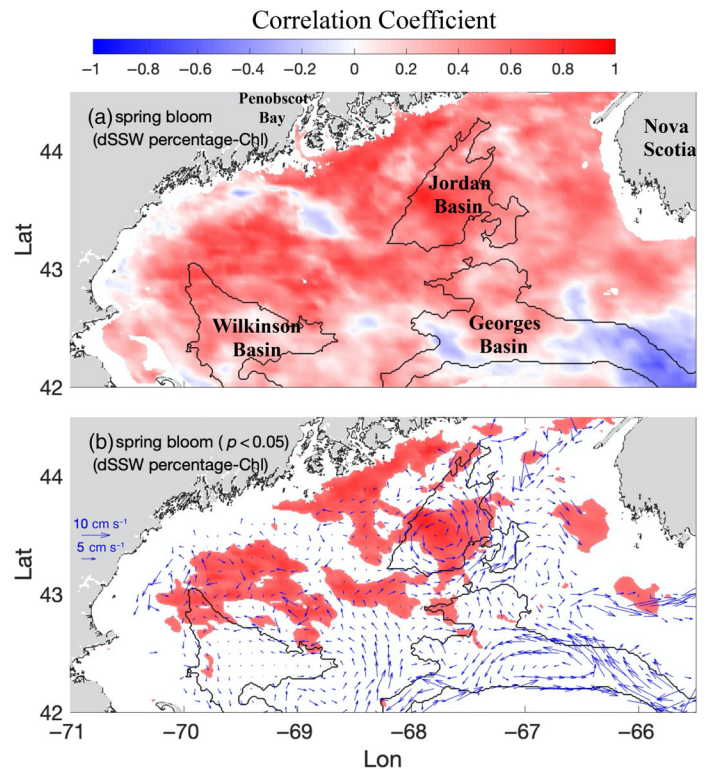


Fig. 4. (a) Spatial distribution of correlation coefficients between dSSW percentage in the deep Northeast Channel and chlorophyll concentration during spring bloom in the GoM. The chlorophyll concentration during the spring bloom in each year is represented by the temporal averaged chlorophyll concentration during the spring blooms identified by the SOM in Fig. 2 (patterns g, h, j, k). (b) The regions where correlation is significant ($p < 0.05$). The blue arrows in (b) demonstrate the FVCOM-GOM3 simulated time- and depth-averaged current field between 100 and 200 m levels from January to May in the GoM. The black contour lines indicate the 200 m isobath.

Estimations of deep-water composition in the NEC and dSSW silicate concentration

We employed the temperature–salinity triangle diagram following Mountain (2012) to quantify the proportions of three deep-water masses entering the GoM through the NEC. The spatial mean temperature and salinity in the NEC were based on the FVCOM-GOM3 model results from January to May (1–3 months prior to the spring bloom; Townsend et al. 2015; Feng et al. 2016; Du et al. 2021). The details of this method are described in Mountain (2012) and the Supporting Information Section S2.

Silicate concentration of dSSW in the NEC is essential in estimating the contribution of dSSW to total new silicate flux into the GoM. However, most previous dSSW silicate measurements were conducted on the Scotian Shelf (Townsend et al. 2010), and directly applying it to our study might underestimate dSSW-related silicate influx because regeneration can enhance silicate concentration from the Scotian Shelf to the NEC (Smith et al. 2012). In this study, we estimated mean

dSSW silicate concentration ($\text{Si}(\text{OH})_4^{\text{SSW}}$) using the following equation:

$$\text{Si}(\text{OH})_4^{\text{mix}} = \text{Si}(\text{OH})_4^{\text{slope}} \times \text{SW}\% + \text{Si}(\text{OH})_4^{\text{SSW}} \times (100\% - \text{SW}\%), \quad (1)$$

where $\text{Si}(\text{OH})_4^{\text{mix}}$ is silicate concentration of newly entered deep waters ($13.33 \mu\text{M}$; Townsend et al. 2010), $\text{Si}(\text{OH})_4^{\text{slope}}$ is mean Slope Water silicate concentration ($12 \mu\text{M}$; Petrie and Yeats 2000; Townsend et al. 2006), and SW% represents the proportion of Slope Water (WSW plus LSW) estimated by the triangle diagram.

Results

SOM patterns of surface chlorophyll

The 12 SOM patterns of surface chlorophyll are shown in the upper panels of Fig. 2, and patterns g, h, j, and k were identified as bloom patterns. Pattern j represented the strongest bloom due to its higher spatial averaged chlorophyll concentration ($g: 1.42 \text{ mg m}^{-3}$; $h: 1.20 \text{ mg m}^{-3}$; $j: 1.91 \text{ mg m}^{-3}$; $k: 1.54 \text{ mg m}^{-3}$). The time series indicated that the spring bloom began in late March/early April, and the peak (pattern j) mainly occurred in April and early May (Fig. 2). Both the time series of BMU and bloom patterns demonstrated the profound interannual variabilities of the spring bloom magnitude and phenological features.

Interannual variabilities of spring bloom magnitude and deep-water composition

The spring bloom magnitude in each year was represented by the spatiotemporally averaged chlorophyll concentration. The results showed that the bloom magnitude declined from 1.88 mg m^{-3} in 2001 to 1.29 mg m^{-3} in 2013, followed by a moderate increase to $\sim 1.55 \text{ mg m}^{-3}$ until 2016 (Fig. 3). Meanwhile, a sharp decline of the dSSW proportion from 38% to 5% occurred between 2001 and 2013 with a slight increase afterward (Fig. 3a). The mean proportion of dSSW in the NEC from 2001 to 2016 was 23.9%. A significant positive correlation was found between the spring bloom magnitude in the GoM and the proportion of dSSW in the NEC ($r = 0.73$; Fig. 3a), suggesting a possible link between dSSW and the spring bloom magnitude. The proportions of two slope water masses (LSW and WSW) were negatively correlated ($r = -0.90$; Fig. 3b), while neither was significantly correlated with the spring bloom magnitude (LSW-bloom: $r = -0.32$; WSW-bloom: $r = -0.01$). To reveal the spatial heterogeneity of dSSW's impact on the spring bloom magnitude, we estimated the correlation between the dSSW proportion in the NEC and the spring bloom magnitude in each grid across the entire GoM (Fig. 4). The results showed an overall positive correlation except for the downstream of the Penobscot Bay and the southeastern GoM (Fig. 4a). The significant correlation coefficients ($p < 0.05$) were mainly distributed along the path of the deep-water inflow (Fig. 4b).

Nutrient regimes in the GoM

The spatial patterns of nitrate and silicate over the top 20 m in spring are shown in Fig. 5a,b. Both nitrate and silicate concentrations were lower in the central GoM and higher

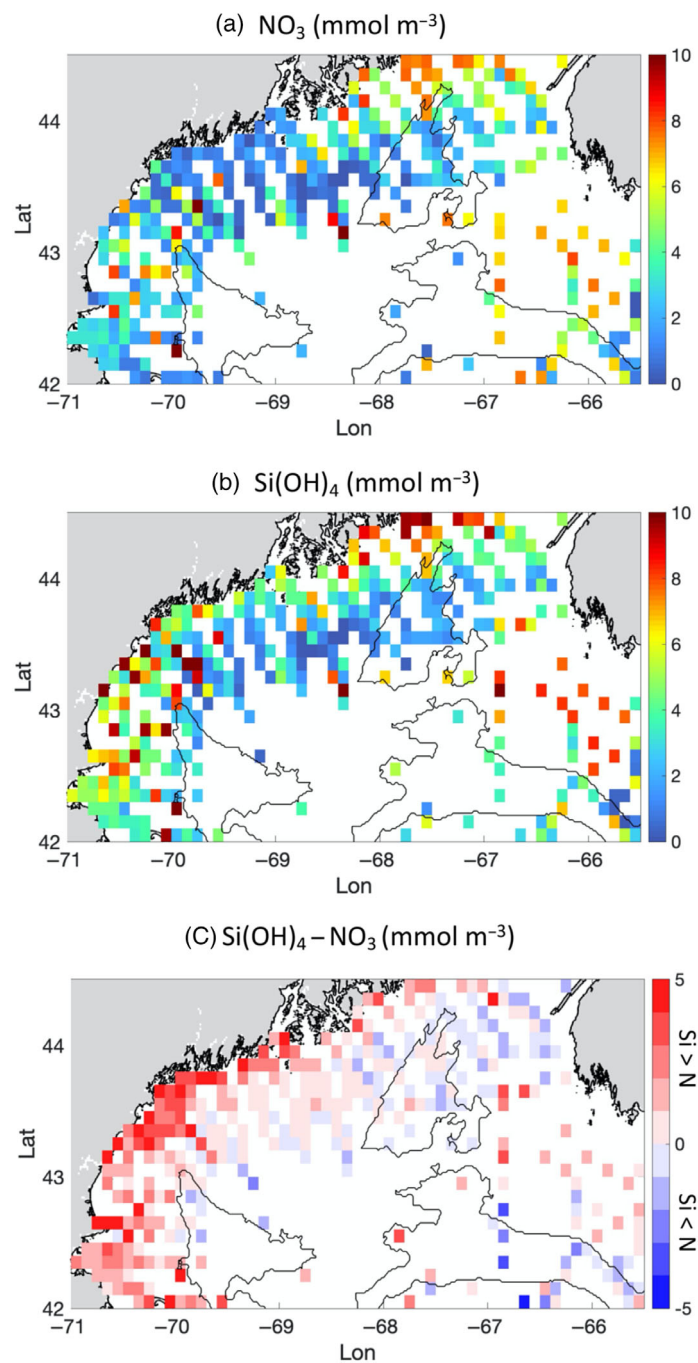


Fig. 5. Nitrate concentration (a), silicate concentration (b), and residual silicate (silicate minus nitrate; c) over the top 20 m in spring (data source: the Gulf of Maine Region Nutrient and Hydrographic Database). The original data are projected onto a grid with $0.1^\circ \times 0.1^\circ$ resolution, and the color in each grid represents the mean value based on all the survey data in the grid. The black contour lines indicate the 200 m isobath.

nearshore. Since diatoms take up nitrate and silicate in roughly equal proportions (Townsend et al. 2006), residual silicate (silicate minus nitrate) was estimated to reveal the primary limiting nutrient in the GoM (Fig. 5c). Positive residual silicate located mostly in nearshore regions, indicating low nitrate concentration limited phytoplankton growth. In the central GoM, negative residual silicate indicated silicate limitation exceeded that of nitrate. The similar spatial distributions of negative residual silicate (Fig. 5c) and dSSW-spring bloom magnitude correlation coefficients (Fig. 4b) suggested that the spring bloom magnitude in the central GoM was associated with silicate-rich dSSW due to stronger silicate limitation.

Deep silicate flux into the GoM through the NEC

The mean deep silicate flux through the NEC from January to May was estimated using along-channel deep-water flux between 100 and 200 m across the transect S1 (see Fig. 1), and mean silicate concentration of newly entered deep waters ($13.33 \mu\text{M}$; Townsend et al. 2010). The deep silicate flux into the GoM was $\sim 2.7 \times 10^8 \text{ mol d}^{-1}$ ($\sim 4.0 \times 10^{10} \text{ mol}$ silicate from January to May). Compared with depth-integrated silicate inventory between 0 and 200 m in the GoM ($\sim 9.9 \times 10^{10} \text{ mol}$) estimated using the World Ocean Atlas dataset (Supporting Information Section S3), deep silicate influx through the NEC from January to May accounted for 40% of silicate inventory in the GoM.

We estimated the dSSW silicate flux across the transect S1 using mean silicate concentration of dSSW, along-channel deep-water flux, and the averaged proportion of dSSW in the NEC (23.9%) estimated above. The mean silicate concentration of dSSW was estimated following Eq. 1, and its value was $\sim 17.56 \mu\text{M}$. The silicate flux associated with dSSW was $\sim 0.8 \times 10^8 \text{ mol d}^{-1}$, which contributed to $\sim 30\%$ of total silicate flux through the NEC.

Discussion

The principal nutrient source supporting primary production in the GoM has been generally thought to be via the influx of Slope Water, and previous studies have emphasized the contributions of different Slope Water components in nutrient supply (Schlitz and Cohen 1984; Ramp et al. 1985; Townsend 1991; Thomas et al. 2003). More recent studies, however, find that the increasing importance of silicate-rich dSSW contributes to the variation of nutrient regime in the GoM (Townsend et al. 2015). As a potentially limiting nutrient in spring, silicate concentration in the GoM is influenced by both external deep-water intrusion and internal recycling (Townsend and Thomas 2002; Townsend et al. 2010; Switzer et al. 2020). The concentration of nitrate, another important nutrient for phytoplankton growth, is modulated by the composition of deep-water inflow and bottom sedimentary denitrification (Christensen et al. 1996; Townsend et al. 2015). The decrease of bottom nitrate concentration from the NEC

to the central GoM indicates that denitrification is important in nitrate removal (Switzer et al. 2020). Quantitative analysis based on a 3D biogeochemical model suggests that denitrification removes $\sim 14 \text{ Gmols yr}^{-1}$ (Zhang et al. 2019). Unlike the depletion of nitrate in the deep water, silicate at depth tends to accumulate from the NEC to the GoM (Christensen et al. 1996; Switzer et al. 2020). The increase of silicate concentration along the deep circulation pathways indicates the importance of silicate recycling in fall (Switzer et al. 2020). However, the significant correlation between the dSSW proportion and the spring bloom magnitude found in this study implies that the dSSW intrusion is more important than internal recycling in modulating silicate concentration in the GoM. A possible reason for such a discrepancy is that the dissolution of diatom cells mainly occurs after the spring blooms, which provides a large number of diatom frustules to the deep water via sinking (Townsend and Thomas 2001; Switzer et al. 2020). In addition, it should be noted that silicate supply might not be the only reason for the correlation between dSSW and the spring bloom magnitude. The distinct hydrographic feature of dSSW (cooler and fresher than the Slope Water) might also influence the spring bloom magnitude by modulating overturning and vertical mixing patterns in the GoM (Christensen and Pringle 2012; Cai et al. 2021). Thus, future work should focus more on the synergistic effects of dSSW-related nutrient and hydrographic conditions on spring bloom dynamics.

The decoupling between the spring bloom magnitude and the dSSW proportion downstream of the Penobscot Bay and the southeastern GoM implies different mechanisms regulating the spring bloom magnitude in these two regions. For the region downstream of the Penobscot Bay, freshwater input with high silicate concentration (up to $200 \mu\text{M}$) is mixed with coastal waters and transported by Western Maine Coastal Current southwestward along the coast, supplying a significant amount of silicate for spring diatom bloom (Schoudel 1996; Anderson et al. 2008). Therefore, nitrate in this region is the primary limiting nutrient during the spring blooms. In the southeastern GoM, the surface nutrient availability can be directly influenced by the offshore oligotrophic surface water rather than deep-water nutrient (Thomas et al. 2003). Given the significant correlation between the spring bloom magnitude in the GoM and the proportion of dSSW in the NEC, it is thus crucial to understand the drivers of dSSW transport into the GoM from upstream. Previous studies have suggested that the dSSW transport from the Scotian Shelf to the GoM is modulated by wind stress (Schwing 1992; Li et al. 2014; Feng et al. 2016), baroclinic forcing (Loder et al. 2001), remote waves (Schwing 1992), and bathymetric variability (Greenberg et al. 1997). The study of Townsend et al. (2015) suggests that the transport of dSSW from the NEC to the Jordan Basin takes about 3 months. If our hypothesized link between the dSSW and the GoM spring bloom remains valid in the future, such a time lag makes it possible to forecast the spring bloom

magnitude in the GoM by monitoring the proportion of dSSW in the NEC during winter and early spring. It is worth noting that not all the deep water in the NEC can be transported into the GoM: part of deep-water mass entering the GoM circulates counterclockwise over the Georges Basin and flows out of the GoM on the western side of the NEC (Ramp et al. 1985; Smith et al. 2001). More recent observations suggest sustained deep outflow during winter, implying the decrease in nutrient supply to the GoM (Smith et al. 2012). The contribution of inflow through the Northern Channel (between Browns Bank and Nova Scotia) to external silicate supply into the GoM was also examined here. Both model results and moored observations suggest that the eastward outflow along Browns Bank's northern flank negatively influences silicate influx into the GoM (Hannah et al. 2001). Moreover, the water flux into the GoM through the Northern Channel decreases with water depth, and the transport direction of silicate-rich deep water mass (depth > 100 m) is outward in winter and spring (Fig. 4b; Hannah et al. 2001). Thus, external nutrient supply into the GoM through the Northern Channel could be much lower than that through the NEC.

Our results also suggest the need to consider adding silicate as a limiting nutrient for the regional ecosystem simulations. Many Nutrient-Phytoplankton-Zooplankton-Detritus models have a sole limiting nutrient (mostly nitrogen) for simulating phytoplankton dynamics (Fennel et al. 2006; Song et al. 2011; Zhang et al. 2019). Such a simplification, however, should be well justified based on the phytoplankton community structure and the objectives of simulations. If the model focuses on the variability of bloom magnitudes controlled largely by diatoms, having silicate as a limiting nutrient becomes essential. Our analyses provide a strong support for a serious consideration of including silicate as a limiting nutrient, and this is particularly important if the focus is on the diatom bloom.

References

- Alvera-Azcárate, A., A. Barth, M. Rixen, and J. M. Beckers. 2005. Reconstruction of incomplete oceanographic data sets using empirical orthogonal functions: Application to the Adriatic Sea surface temperature. *Ocean Model.* **9**: 325–346. doi:10.1016/j.ocemod.2004.08.001
- Alvera-Azcárate, A., A. Barth, J. M. Beckers, and R. H. Weisberg. 2007. Multivariate reconstruction of missing data in sea surface temperature, chlorophyll, and wind satellite fields. *J. Geophys. Res. Ocean* **112**: 1–11. doi:10.1029/2006JC003660
- Alvera-Azcárate, A., A. Barth, D. Sirjacobs, F. Lenartz, and J. M. Beckers. 2011. Data interpolating empirical orthogonal functions (DINEOF): A tool for geophysical data analyses. *Mediterr. Mar. Sci.* **12**: 5–11. doi:10.12681/mms.64
- Anderson, D. M., J. M. Burkholder, W. P. Cochlan, P. M. Glibert, C. J. Gobler, C. A. Heil, R. M. Kudela, M. L. Parsons, J. E. J. Rensel, D. W. Townsend, V. L. Trainer, and G. A. Vargo. 2008. Harmful algal blooms and eutrophication: Examining linkages from selected coastal regions of the United States. *Harmful Algae* **8**: 39–53. doi:10.1016/j.hal.2008.08.017
- Beckers, J. M., and M. Rixen. 2003. EOF calculations and data filling from incomplete oceanographic datasets. *J. Atmos. Oceanic Tech.* **20**: 1839–1856. doi:10.1175/1520-0426(2003)020<1839:ECADFF>2.0.CO;2.
- Bigelow, H. B. 1927. Physical oceanography of the Gulf of Maine. *Bull. U.S. Bur. Fish.* **40**: 511–1027.
- Brown, W. S., and J. D. Irish. 1993. The annual variation of water mass structure in the Gulf of Maine: 1986–1987. *J. Mar. Res.* **51**: 53–107. doi:10.1357/0022240933223828
- Brzezinski, M. A. 1985. The Si:C:N ratio of marine diatoms: Interspecific variability and the effect of some environmental variables 1. *J. Phycol.* **21**: 347–357.
- Cai, C., Y.-O. Kwon, Z. Chen, and P. Fratantoni. 2021. Mixed layer depth climatology over the northeast US continental shelf (1993–2018). *Cont. Shelf Res.* **231**: 104611. doi:10.1016/j.csr.2021.104611
- Chen, C., H. Liu, and R. C. Beardsley. 2003. An unstructured grid, finite-volume, three-dimensional, primitive equations ocean model: Application to coastal ocean and estuaries. *J. Atmos. Oceanic Tech.* **20**: 159–186. doi:10.1175/1520-0426(2003)020<0159:AUGFVT>2.0.CO;2.
- Chen, C., P. Malanotte-Rizzoli, J. Wei, R. C. Beardsley, Z. Lai, P. Xue, S. Lyu, Q. Xu, J. Qi, and G. W. Cowles. 2009. Application and comparison of kalman filters for coastal ocean problems: An experiment with FVCOM. *J. Geophys. Res. Ocean* **114**: C05011. doi:10.1029/2007JC004548
- Chen, C., H. Huang, R. C. Beardsley, Q. Xu, R. Limeburner, G. W. Cowles, Y. Sun, J. Qi, and H. Lin. 2011. Tidal dynamics in the Gulf of Maine and New England shelf: An application of FVCOM. *J. Geophys. Res. Ocean* **116**: C12010. doi:10.1029/2011JC007054
- Chen, C., Z. Lin, R. C. Beardsley, T. Shyka, Y. Zhang, Q. Xu, J. Qi, H. Lin, and D. Xu. 2021a. Impacts of sea level rise on future storm-induced coastal inundations over Massachusetts coast. *Nat. Hazards* **106**: 375–399. doi:10.1007/s11069-020-04467-x
- Chen, C., L. Zhao, S. Gallagher, R. Ji, P. He, C. Davis, R. C. Beardsley, D. Hart, W. C. Gentleman, L. Wang, S. Li, H. Lin, K. Stokesbury, and D. Bethoney. 2021b. Impact of larval behaviors on dispersal and connectivity of sea scallop larvae over the northeast U.S. shelf. *Prog. Oceanogr.* **195**: 102604. doi:10.1016/j.pocean.2021.102604
- Christensen, J. P., D. W. Townsend, and J. P. Montoya. 1996. Water column nutrients and sedimentary denitrification in the Gulf of Maine. *Cont. Shelf Res.* **16**: 489–515. doi:10.1016/0278-4343(95)00027-5
- Christensen, M. K., and J. M. Pringle. 2012. The frequency and cause of shallow winter mixed layers in the Gulf of Maine. *J. Geophys. Res. Ocean* **117**. doi:10.1029/2011JC007358
- Du, J., W. G. Zhang, and Y. Li. 2021. Variability of deep water in Jordan Basin of the Gulf of Maine: Influence of Gulf Stream Warm Core Rings and the Nova Scotia Current.

- J. Geophys. Res. Ocean **126**: e2020JC017136. doi:[10.1029/2020jc017136](https://doi.org/10.1029/2020jc017136)
- Durbin, E. G., Campbell, R. G., Casas, M. C., Ohman, M. D., Niehoff, B., Runge, J., Wagner, M. 2003. Interannual variation in phytoplankton blooms and zooplankton productivity and abundance in the Gulf of Maine during winter. *Marine Ecology Progress Series*. **254**: 81–100. doi:[10.3354/meps254081](https://doi.org/10.3354/meps254081)
- Feng, H., D. Vandemark, and J. Wilkin. 2016. Gulf of Maine salinity variation and its correlation with upstream Scotian Shelf currents at seasonal and interannual time scales. *J. Geophys. Res. Ocean*. **121**: 8585–8607. doi:[10.1002/2016JC012337](https://doi.org/10.1002/2016JC012337)
- Fennel, K., J. Wilkin, J. Levin, J. Moisan, J. O'Reilly, and D. Haidvogel. 2006. Nitrogen cycling in the Middle Atlantic Bight: Results from a three-dimensional model and implications for the North Atlantic nitrogen budget. *Global Biogeochem. Cycl.* **20**: GB3007. doi:[10.1029/2005GB002456](https://doi.org/10.1029/2005GB002456)
- Gatien, M. G. 1976. A study in the slope water region south of Halifax. *J. Fish. Board Canada* **33**: 2213–2217.
- Greenberg, D. A., J. W. Loder, Y. Shen, D. R. Lynch, and C. E. Naimie. 1997. Spatial and temporal structure of the barotropic response of the Scotian Shelf and Gulf of Maine to surface wind stress: A model-based study. *J. Geophys. Res. Ocean* **102**: 20897–20915. doi:[10.1029/97JC00442](https://doi.org/10.1029/97JC00442)
- Hannah, C. G., J. A. Shore, and J. W. Loder. 2001. Seasonal circulation on the Western and Central Scotian Shelf. *J. Phys. Oceanogr.* **31**: 591–615 doi:[10.1175/1520-0485\(2001\)031<0591:SCOTWA>2.0.CO;2](https://doi.org/10.1175/1520-0485(2001)031<0591:SCOTWA>2.0.CO;2).
- Ji, R., Z. Feng, B. T. Jones, C. Thompson, C. Chen, N. R. Record, and J. A. Runge. 2017. Coastal amplification of supply and transport (CAST): A new hypothesis about the persistence of *Calanus finmarchicus* in the Gulf of Maine. *ICES J. Mar. Sci.* **74**: 1865–1874. doi:[10.1093/icesjms/fsw253](https://doi.org/10.1093/icesjms/fsw253)
- Kohonen, T. 2001, *Self-organizing maps*, 3rd Edition., Springer Series in Information Sciences, 501 pp. Springer.
- Kohonen, T. 1982. Self-organized formation of topologically correct feature maps. *Biol. Cybern.* **43**: 59–69. doi:[10.1007/BF00337288](https://doi.org/10.1007/BF00337288)
- Li, Y., R. Ji, P. S. Fratantoni, C. Chen, J. A. Hare, C. S. Davis, and R. C. Beardsley. 2014. Wind-induced interannual variability of sea level slope, along-shelf flow, and surface salinity on the Northwest Atlantic shelf. *J. Geophys. Res. Ocean* **119**: 2462–2479. doi:[10.1002/2013JC009385](https://doi.org/10.1002/2013JC009385)
- Li, Y., P. S. Fratantoni, C. Chen, J. A. Hare, Y. Sun, R. C. Beardsley, and R. Ji. 2015. Spatio-temporal patterns of stratification on the Northwest Atlantic shelf. *Prog. Oceanogr.* **134**: 123–137. doi:[10.1016/j.pocean.2015.01.003](https://doi.org/10.1016/j.pocean.2015.01.003)
- Liu, Y., and R. H. Weisberg. 2005. Patterns of ocean current variability on the West Florida Shelf using the self-organizing map. *J. Geophys. Res. Ocean* **110**: C06003. doi:[10.1029/2004JC002786](https://doi.org/10.1029/2004JC002786)
- Liu, Y., R. H. Weisberg, and C. N. K. Mooers. 2006. Performance evaluation of the self-organizing map for feature extraction. *J. Geophys. Res. Ocean* **111**: C05018. doi:[10.1029/2005JC003117](https://doi.org/10.1029/2005JC003117)
- Liu, Y., P. MacCready, and B. M. Hickey. 2009. Columbia River plume patterns in summer 2004 as revealed by a hindcast coastal ocean circulation model. *Geophys. Res. Lett.* **36**: L02601. doi:[10.1029/2008GL036447](https://doi.org/10.1029/2008GL036447)
- Liu, Y., and R. H. Weisberg. 2011. A review of self-organizing map applications in meteorology and oceanography. In J. I. Mwasiagi [ed.], *Self-organizing map—Applications and novel algorithm design*. InTech.
- Liu, Y., R. H. Weisberg, J. M. Lenes, L. Zheng, K. Hubbard, and J. J. Walsh. 2016. Offshore forcing on the “pressure point” of the West Florida Shelf: Anomalous upwelling and its influence on harmful algal blooms. *J. Geophys. Res. Oceans* **121**: 5501–5515. doi:[10.1038/175238c0](https://doi.org/10.1038/175238c0)
- Loder, J. W., J. A. Shore, C. G. Hannah, and B. D. Petrie. 2001. Decadal-scale hydrographic and circulation variability in the Scotia—Maine region. *Deep. Res. Part II Top. Stud. Oceanogr.* **48**: 3–35. doi:[10.1016/S0967-0645\(00\)00080-1](https://doi.org/10.1016/S0967-0645(00)00080-1)
- Mountain, D. G. 2012. Labrador slope water entering the Gulf of Maine—response to the North Atlantic Oscillation. *Cont. Shelf Res.* **47**: 150–155. doi:[10.1016/j.csr.2012.07.008](https://doi.org/10.1016/j.csr.2012.07.008)
- Pan, X., A. Mannino, H. G. Marshall, K. C. Filippino, and M. R. Mulholland. 2011. Remote sensing of phytoplankton community composition along the northeast coast of the United States. *Remote Sens. Environ.* **115**: 3731–3747. doi:[10.1016/j.rse.2011.09.011](https://doi.org/10.1016/j.rse.2011.09.011)
- Pershing, A. J., Stamieszkin, K. 2020. The North Atlantic Ecosystem, from Plankton to Whales. *Annual Review of Marine Science.* **12**(1): 339–359. doi:[10.1146/annurev-marine-010419-010752](https://doi.org/10.1146/annurev-marine-010419-010752)
- Petrie, B., and P. Yeats. 2000. Annual and interannual variability of nutrients and their estimated fluxes in the Scotian Shelf-Gulf of Maine region. *Can. J. Fish. Aquat. Sci.* **57**: 2536–2546. doi:[10.1139/f00-235](https://doi.org/10.1139/f00-235)
- Platt, T., Fuentes-Yaco, C., Frank, K. T. 2003. Spring algal bloom and larval fish survival. *Nature.* **423**(6938): 398–399. doi:[10.1038/423398b](https://doi.org/10.1038/423398b)
- Ramp, S. R., R. J. Schlitz, and W. R. Wright. 1985. The deep flow through the Northeast Channel, Gulf of Maine. *J. Phys. Oceanogr.* **15**: 1790–1808 doi:[10.1175/1520-0485\(1985\)015<1790:TDFTTN>2.0.CO;2](https://doi.org/10.1175/1520-0485(1985)015<1790:TDFTTN>2.0.CO;2).
- Rebuck, N. D., and D. W. Townsend. 2014. A climatology and time series for dissolved nitrate in the Gulf of Maine region. *Deep. Res. Part II Top. Stud. Oceanogr.* **103**: 223–237. doi:[10.1016/j.dsr2.2013.09.006](https://doi.org/10.1016/j.dsr2.2013.09.006)
- Saba, V. S., K. J. W. Hyde, N. D. Rebuck, K. D. Friedland, J. A. Hare, M. Kahru, and M. J. Fogarty. 2015. Physical associations to spring phytoplankton biomass interannual variability in the U.S. Northeast Continental Shelf. *J. Geophys. Res. Biogeo.* **120**: 205–220. doi:[10.1038/175238c0](https://doi.org/10.1038/175238c0)
- Schlitz, R. J., and E. B. Cohen. 1984. A nitrogen budget for the Gulf of Maine and Georges Bank. *Biol. Ocean* **3**: 203–222.
- Schoudel, A., 1996. The seasonal variation of nutrients in three Maine estuaries. M.Sc. thesis, Univ. of New Hampshire, Durham, NH, 103 pp.

- Schwing, F. B. 1992. Subtidal response of Scotian Shelf circulation to local and remote forcing. Part I Observations. *J. Phys. Oceanogr.* **22**: 523–541.
- Smith, P. C., R. W. Houghton, R. G. Fairbanks, and D. G. Mountain. 2001. Interannual variability of boundary fluxes and water mass properties in the Gulf of Maine and on Georges Bank: 1993–1997. *Deep. Res. Part II Top. Stud. Oceanogr.* **48**: 37–70. doi:[10.1016/S0967-0645\(00\)00081-3](https://doi.org/10.1016/S0967-0645(00)00081-3)
- Smith, P. C., N. R. Pettigrew, P. Yeats, D. W. Townsend, and G. Han. 2012. Regime shift in the Gulf of Maine. *Am. Fish. Soc. Symp.* **79**: 185–203.
- Song, H., R. Ji, C. Stock, K. Kearney, and Z. Wang. 2011. Interannual variability in phytoplankton blooms and plankton productivity over the Nova Scotian Shelf and in the Gulf of Maine. *Mar. Ecol. Prog. Ser.* **426**: 105–118. doi:[10.3354/meps09002](https://doi.org/10.3354/meps09002)
- Sun, Y., C. Chen, R. C. Beardsley, Q. Xu, J. Qi, and H. Lin. 2013. Impact of current-wave interaction on storm surge simulation: A case study for Hurricane Bob. *J. Geophys. Res. Ocean* **118**: 2685–2701. doi:[10.1002/jgrc.20207](https://doi.org/10.1002/jgrc.20207)
- Sun, Y., C. Chen, R. C. Beardsley, D. Ullman, B. Butman, and H. Lin. 2016. Surface circulation in Block Island Sound and adjacent coastal and shelf regions: A FVCOM-CODAR comparison. *Prog. Oceanogr.* **143**: 26–45. doi:[10.1016/j.pocean.2016.02.005](https://doi.org/10.1016/j.pocean.2016.02.005)
- Switzer, M. E., D. W. Townsend, and N. R. Pettigrew. 2020. The effects of source water masses and internal recycling on concentrations of dissolved inorganic nutrients in the Gulf of Maine. *Cont. Shelf Res.* **204**: 104157. doi:[10.1016/j.csr.2020.104157](https://doi.org/10.1016/j.csr.2020.104157)
- Telszewski, M., A. Chazottes, U. Schuster, A. J. Watson, C. Moulin, D. C. E. Bakker, M. González-Dávila, T. Johannessen, A. Körtzinger, H. Lüger, A. Olsen, A. Omar, X. A. Padin, A. F. Ríos, T. Steinhoff, M. Santana-Casiano, D. W. R. Wallace, and R. Wanninkhof. 2009. Estimating the monthly pCO₂ distribution in the North Atlantic using a self-organizing neural network. *Biogeosciences* **6**: 1405–1421. doi:[10.5194/bg-6-1405-2009](https://doi.org/10.5194/bg-6-1405-2009)
- Thomas, A. C., D. W. Townsend, and R. Weatherbee. 2003. Satellite-measured phytoplankton variability in the Gulf of Maine. *Cont. Shelf Res.* **23**: 971–989. doi:[10.1016/S0278-4343\(03\)00086-4](https://doi.org/10.1016/S0278-4343(03)00086-4)
- Townsend, D. W. 1991. Influences of oceanographic processes on the biological productivity of the Gulf of Maine. *Rev. Aquat. Sci.* **5**: 211–230.
- Townsend, D. W. 1998. Sources and cycling of nitrogen in the Gulf of Maine. *J. Mar. Syst.* **16**: 283–295. doi:[10.1016/S0924-7963\(97\)00024-9](https://doi.org/10.1016/S0924-7963(97)00024-9)
- Townsend, D. W., and A. C. Thomas. 2001. Winter-spring transition of phytoplankton chlorophyll and inorganic nutrients on Georges Bank. *Deep. Res. Part II Top. Stud. Oceanogr.* **48**: 199–214. doi:[10.1016/S0967-0645\(00\)00119-3](https://doi.org/10.1016/S0967-0645(00)00119-3)
- Townsend, D. W., and M. Thomas. 2002. Springtime nutrient and phytoplankton dynamics on Georges Bank. *Mar. Ecol. Prog. Ser.* **228**: 57–74. doi:[10.3354/meps228057](https://doi.org/10.3354/meps228057)
- Townsend, D. W., N. R. Pettigrew, and A. C. Thomas. 2005. On the nature of Alexandrium fundyense blooms in the Gulf of Maine. *Deep. Res. Part II Top. Stud. Oceanogr.* **52**: 2603–2630. doi:[10.1016/j.dsr2.2005.06.028](https://doi.org/10.1016/j.dsr2.2005.06.028)
- Townsend, D. W., A. C. Thomas, L. M. Mayer, M. A. Thomas, and J. A. Quinlan. 2006. Oceanography of the Northwest Atlantic continental shelf, p. 119–168. *In* A. R. Robinson and K. H. Brink [eds.], *The Sea*, v. **14**. Cambridge MA: Harvard Univ. Press.
- Townsend, D. W., N. D. Rebeck, M. A. Thomas, L. Karp-Boss, and R. M. Gettings. 2010. A changing nutrient regime in the Gulf of Maine. *Cont. Shelf Res.* **30**: 820–832. doi:[10.1016/j.csr.2010.01.019](https://doi.org/10.1016/j.csr.2010.01.019)
- Townsend, D. W., N. R. Pettigrew, M. A. Thomas, M. G. Neary, D. J. McGillicuddy, and J. O'Donnell. 2015. Water masses and nutrient sources to the Gulf of Maine. *J. Mar. Res.* **73**: 93–122. doi:[10.1357/002224015815848811](https://doi.org/10.1357/002224015815848811)
- Townsend, D. W., Cammen, L. M. 1988. Potential importance of the timing of spring plankton blooms to benthic-pelagic coupling and recruitment of juvenile demersal fishes. *Biol. Oceanogr.* **5**: 215–228.
- Turner, K. J., C. B. Mouw, K. J. W. Hyde, R. Morse, and A. B. Ciochetto. 2021. Optimization and assessment of phytoplankton size class algorithms for ocean color data on the Northeast U.S. continental shelf. *Remote Sens. Environ.* **267**: 112729. doi:[10.1016/j.rse.2021.112729](https://doi.org/10.1016/j.rse.2021.112729)
- Zang, Z., R. Ji, Z. Feng, C. Chen, S. Li, and C. S. Davis. 2021. Spatially varying phytoplankton seasonality on the Northwest Atlantic shelf: A model-based assessment of patterns, drivers, and implications. *ICES J. Mar. Sci.* **78**: 1920–1934. doi:[10.1093/icesjms/fsab102](https://doi.org/10.1093/icesjms/fsab102)
- Zhang, S., C. A. Stock, E. N. Curchitser, and R. Dussin. 2019. A numerical model analysis of the mean and seasonal nitrogen budget on the Northeast U.S. Shelf. *J. Geophys. Res. Ocean* **124**: 2969–2991. doi:[10.1029/2018JC014308](https://doi.org/10.1029/2018JC014308)

Acknowledgments

This study was supported by NOAA Coastal and Ocean Climate Application (COCA) Program (NA17OAR4310273) and NSF Northeast US Shelf-Long-Term Ecological Research (NES-LTER) Program (OCE-1655686). This study greatly benefited from discussions with the NES-LTER team members, Dr. David W. Townsend at the University of Maine and Dr. Aida Alvera-Azcárate at the University of Liège.

Submitted 24 July 2021

Revised 21 December 2021

Accepted 07 February 2022